Fabric Evolution in Granular Materials Under Strain Probing

Mehdi Pouragha[1], Niels P. Kruyt[2], and Richard Wan[1(✉)]

[1] Civil Engineering Department, University of Calgary, Calgary, Canada
{mpouragh,wan}@ucalgary.ca
[2] Department of Mechanical Engineering,
University of Twente, Enschede, The Netherlands
n.p.kruyt@utwente.nl

Abstract. The fabric of granular materials, as the underlying internal contact network through which the interparticle forces transmit the stress, plays a key role in describing their elasticity, critical state, and dilatancy, to name a few. Just as response envelopes have been developed by Gudehus back in 1979 to get an overall picture of constitutive models and the nature of constitutive equations, herein, the evolution of contact fabric in granular materials when subjected to strain probes is explored through series of Discrete Element Method (DEM) simulations. As the first study of its kind, and also due to the richness of the observed responses, the scope of the study has been limited to isotropic configurations. The contribution of contact loss, gain, and reorientation mechanisms to the changes in the associated second order fabric tensor has been investigated as the proportion of vertical to horizontal strain changed during a strain probing procedure. Intriguingly, the evolution of fabric with strain probes shows a strong asymmetry in compression and extension, signalling an incrementally nonlinear relation between fabric and strain increments, despite the incrementally linear elastic stress-strain response. Such results suggest that the origins of the incrementally nonlinear stress-strain responses often observed in later stages of deviatoric loading of granular materials can be potentially traced back to characteristics of fabric evolution.

1 Introduction

The micromechanical study of granular materials encompasses the underlying connections between the microscopic-particle scales and the various characteristics at the macroscopic-continuum level with interparticle contacts as the main focus. Micromechanical descriptions of stress [1,9,19,30,36] and strain [2,14], and dilatancy in particular [4,15,16,35], show the important role that the internal contacts arrangement play in relating variables across the different scales. Therefore, having a detailed understanding of contact evolution during mechanical loading is essential in formulating micromechanics-based constitutive models for granular materials [10,17,18,32,37].

W. Wu (Ed.): *Desiderata Geotechnica*, SSGG, pp. 151–161, 2019.
https://doi.org/10.1007/978-3-030-14987-1_19

The internal contact configuration is often characterized by a second order fabric tensor [22,31] describing: the principal directions of contacts, the average number of contacts per particle, or coordination number, and the fabric anisotropy which quantifies the deviation of the fabric tensor from isotropy.

In fact, it is desirable to connect stress to strain through both coordination number and fabric anisotropy as worked out in [24,26] to arrive at so-called stress-strain-fabric relations for different stages of loading. The embedment of microstructural information can done through a statistical analysis of the micromechanical expression for the average stress tensor [9,19,36], relating interparticle contact forces to branch vectors that connect centroids of particles in contact as given by Rothenburg and coworkers [29,30], and the more recent studies on particle kinematics [13,15,23,34].

The question of how contact fabric evolves has been addressed in previous studies, see [13] for a thorough review. In general, two classes of studies can be recognized based on whether fabric evolution is related to stress [21] or to strain [6,13,27,28] increments. More recent studies suggest that a combination of stress and strain controls the evolution of fabric, with contact loss and gain being related to forces and deformations, respectively [25].

Nonetheless, the previous literature mostly studies the fabric evolution under simple conventional loading paths, such as in biaxial, triaxial, or isochoric tests. As such, the generality of such studies is considerably limited, recalling that the elasto-plastic response of granular materials is incremental in nature and generally depends upon the direction of loading [7,8,20,33]. Such a direction dependence, or incremental nonlinearity, is often studied via directional probing; a pioneer method also known as Gudehus envelope [11], where vertical and horizontal stress (or strain) increments in varying ratios are applied to the granular assembly, while the magnitude of the applied loading increment is kept constant [3,5].

The current study investigates the evolution of contact fabric in response to directional strain probes. As a first step toward this topic, the direction dependence of the fabric response is investigated herein for isotropic, two-dimensional granular assemblies with different initial coordination numbers. Discrete Element Method (DEM for short) simulations have been performed to measure various contributions to the evolution of the fabric tensor due to the contact loss, gain, and reorientation mechanisms. The results exhibit a strong *incrementally nonlinear* evolution of fabric tensor, that is in stark contrast with the accompanying elastic, linear stress-strain response. Such directional dependencies of fabric response, serves as a precursor for an elasto-plastic stress-strain response, normally reflected as the dependency of the stress response on the direction of loading.

2 Micromechanics

The internal structure of the interparticle contact network, is often characterized by a second-order fabric tensor $\boldsymbol{F}$ encompassing the density and the directional distribution of contact as [12,22,31]:

$$F_{ij} = \frac{2}{N_p} \sum_{c \in \mathbb{C}} n_i^c \, n_j^c \tag{1}$$

with N_p being the number of particles (excluding rattlers, i.e. particles with fewer than two contacts), $\mathbb{C}$ the set of all contacts, and $\boldsymbol{n}^c$ the contact normal vector at contact c.

The characteristics of the fabric tensor are herein studied in terms of two prominent variables: the coordination number, Z, defined as the average number of contacts per particle, and an anisotropy measure, A, both defined in terms of the principal values F_1 and F_2 of the fabric tensor $\boldsymbol{F}$:

$$Z = \frac{2N_c}{N_p} = \mathrm{tr}(\boldsymbol{F}) = F_1 + F_2, \quad A = F_1 - F_2 \tag{2}$$

where N_c is the total number of contacts. The commonly used fabric anisotropy, see e.g. [30], is related to these two variable by $2A = a_c \, Z$.

The change in fabric tensor can be decomposed into additive contributions from three mechanisms: contact gain, contact loss, and contact reorientation [13,25], i.e.

$$\begin{aligned} \Delta F_{ij} &= \frac{2}{N_p} \Big(\sum_{c \in \mathbb{C}^{\mathrm{final}}} n_i^c \, n_j^c - \sum_{c \in \mathbb{C}^{\mathrm{init}}} n_i^c \, n_j^c \Big) \\ &= \frac{2}{N_p} \sum_{c \in \Delta\mathbb{C}^g} n_i^c \, n_j^c - \frac{2}{N_p} \sum_{c \in \Delta\mathbb{C}^l} n_i^c \, n_j^c + \frac{2}{N_p} \sum_{c \in \mathbb{C}^r} \Delta(n_i^c \, n_j^c) \\ &= \quad \Delta F_{ij}^g \quad - \quad \Delta F_{ij}^l \quad + \quad \Delta F_{ij}^r \end{aligned} \tag{3}$$

with the sets of lost and gained contacts denoted by $\Delta\mathbb{C}^l$ and $\Delta\mathbb{C}^g$ respectively, while $\mathbb{C}^r$ is the set of persisting contacts.

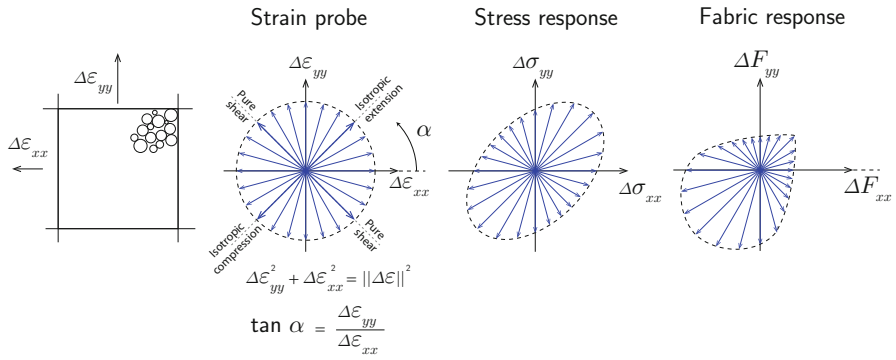

Fig. 1. Schematics of strain probe, stress response and fabric response.

As mentioned earlier, previous studies such as [13,25] have indeed provided insights as to how the fabric tensor changes due to these mechanisms along single monotonic loading (stress or strain) paths. The scope of the investigation is

broadened here by exploring the evolution of the fabric tensor in response to different proportional loading paths through strain probes, as illustrated schematically in Fig. 1. As a first step towards the study of more complex anisotropic systems, the current work is restricted to isotropic initial samples.

3 DEM Simulations

DEM simulations have been performed on two-dimensional square assemblies of 50,000 circular particles with uniformly distributed radii and a ratio of maximum to minimum particle radii of $r_{\max}/r_{\min} = 2$. Similar linear contact stiffnesses have been set for normal and tangential directions, $k_n = k_t$, with the relative stiffness of $k_n/p_0 = 5 \times 10^3$, where p_0 is the initial confining pressure. The interparticle friction has been set at $\mu = 0.5$.

In order to also investigate the effect of the initial coordination number, six initial samples, with varying coordination numbers, Z_0, and void ratios, e_0, were prepared, as listed in Table 1. The sample preparation method has been carefully chosen to yield initially isotropic samples with the initial fabric anisotropy remaining $|a_{c0}| \leq 10^{-4}$. After stabilizing the sample under the initial confining stress, strain probes with a magnitude of $||\Delta\boldsymbol{\varepsilon}|| = \sqrt{\Delta\varepsilon_{yy}^2 + \Delta\varepsilon_{xx}^2} = 2 \times 10^{-4}$ were applied to the samples.

Table 1. Coordination number Z_0 and void ratio e_0, after compaction, of the initial samples.

Z_0	4.53	4.21	4.10	3.87	3.76	3.68
e_0	0.157	0.173	0.179	0.196	0.204	0.211

Figure 2 presents the stress and fabric incremental responses to the imposed strain probes for the dense sample with initial coordination number of $Z_0 = 4.53$. Normal contact stiffness k_n has been used as a scaling factor to render stresses dimensionless.

While the common symmetry around $\alpha = 45°$, expected for an isotropic material, is observed, it is clear that the fabric response is incrementally nonlinear with respect to the strain increment as the symmetry breaks down around $\alpha = 135°$, i.e. contact loss in pure extension does not match the contact gain in pure compression.

The stress responses of samples to the strain probes of the same size are shown in Fig. 3. To avoid overcrowding, only the final states of strain and stress increments are plotted. Furthermore, the total strain was decomposed into elastic and plastic parts by repeating probes with an artificially large interparticle friction to suppress any sliding mechanism [26]. This showed that plastic deformations were insignificant (<1%), hence the total strains can be considered as elastic.

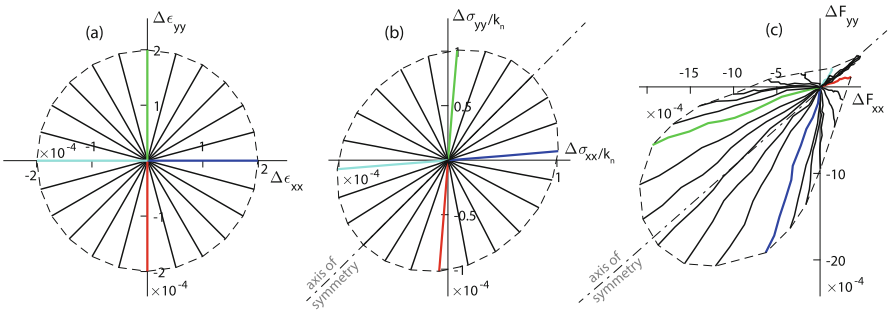

Fig. 2. (a) Imposed strain probes, (b) stress responses, and (c) fabric responses. Results for the dense sample with initial coordination number $Z_0 = 4.53$. Some characteristic probe directions are shown in colour for easy interpretation and clarity.

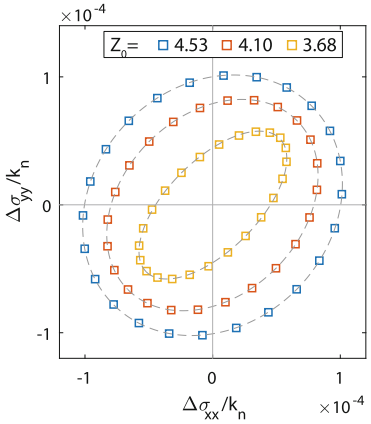

Fig. 3. Dimensionless stress responses to the strain probes with magnitude of $||\Delta\varepsilon|| = 2 \times 10^{-4}$ for samples with different (selected) initial coordination numbers Z_0. Only the final points of the stress response have been plotted. The dashed lines represent elliptical fits that correspond to an incrementally linear stress response.

The contact configuration at the beginning and at the end of the strain probes can be compared to compute the fabric change due contact loss, gain, and reorientation mechanisms, $\Delta\boldsymbol{F}^l$, $\Delta\boldsymbol{F}^g$, and $\Delta\boldsymbol{F}^r$, as defined in Eq. 3. While not presented here, the results indicate that the principal directions of these tensors are aligned with the horizontal and vertical directions. Therefore, the properties of these tensors are reduced to the sum of, and difference between their vertical and horizontal components (which are principal values). For generality, the results are normalized to the strain probe magnitude $||\Delta\boldsymbol{\varepsilon}||$ which presents the rate of change with respect to strain increment:

$$\Delta Z^{*m} = \frac{\Delta F^{m}_{yy} + \Delta F^{m}_{xx}}{||\Delta \boldsymbol{\varepsilon}||} = \Delta F^{*m}_{yy} + \Delta F^{*m}_{xx}$$
$$\Delta A^{*m} = \frac{\Delta F^{m}_{yy} - \Delta F^{m}_{xx}}{||\Delta \boldsymbol{\varepsilon}||} = \Delta F^{*m}_{yy} - \Delta F^{*m}_{xx} \qquad (4)$$
$$m = l,\ g,\ r \quad \text{for contact loss, gain, and reorientation}$$

with the parameter ΔZ^{*m} in Eq. 4 denoting the rate of change in coordination number due to each mechanism, while ΔA^{*m} is related to the associated rate of change of fabric anisotropy. It should be noticed that the variable ΔA^{*m} in Eq. 4 is defined such that, depending on the direction of the maximum fabric change, it can assume both positive and negative values. Figure 4 shows the variation of ΔZ^{*m} and ΔA^{*m} with probe direction α for the probes presented in Fig. 3.

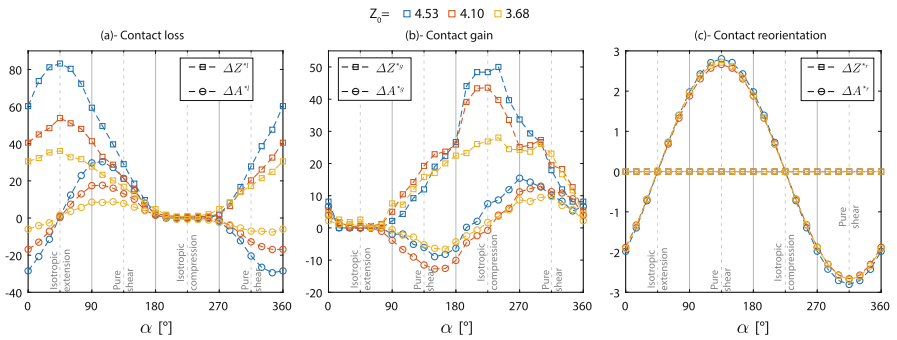

Fig. 4. Rate of change in contact fabric tensor due to (a) contact loss, (b) contact gain, and (c) contact reorientation, as defined in Eq. 3 for strain probes shown in Fig. 3. The square symbols show the sum of the vertical and horizontal (principal) components of the tensors, and the circles show the difference between these two values, as defined in Eq. 4.

The results in Fig. 4 indicate that the rate of contact loss in isotropic extension does not match the rate of contact gain in isotropic compression, which leads to the asymmetry of fabric change around $\alpha = 135°$, as already observed in Fig. 2(c). By definition, no coordination number change is associated with contact reorientation, i.e. $\Delta Z^{*r} = 0$. Moreover, the contribution of contact reorientation to fabric change remains negligible compared to contact loss and gain. While no clear dependency on initial coordination number is observed for the contact reorientation in Fig. 4(c), both variables ΔZ^{*m} and ΔA^{*m} for contact gain and loss mechanisms exhibit an increase as initial coordination number Z_0 increases, as shown in Fig. 4(a) and (b).

Furthermore, the results in Figs. 4(a) and (b) indicate that the maximum change in fabric anisotropy parameter, ΔA^{*m}, does not occur for the directions of pure shear, $\alpha = 135°$ and $315°$. Instead, the directions of these extrema are

shifted slightly towards the extension half region of the probes, i.e. $-45° < \alpha < 135°$. As such, it is concluded that the largest change in fabric anisotropy occurs for a strain probe direction that involves a combination of deviatoric and extension strain.

3.1 Analysis of DEM Results with Representation Theorem

Following the representation theorem for the functional dependence of a second-order tensor on another second-order tensor in two-dimensional isotropic systems, the change in fabric due to each mechanism can be readily expressed as:

$$\Delta F_{ij}^{*m} = \psi_1^m \delta_{ij} + \psi_2^m \Delta \varepsilon_{ij}^*, \quad m = l,\, g,\, r \tag{5}$$

where ψ_1^m and ψ_2^m are functions of the invariants of $\Delta\boldsymbol{\varepsilon}^*$ as well as the initial coordination number, Z_0. Assuming Fourier series expansion up to the second order of the probe direction, the expression in Eq. 5 can be reformulated in terms of ΔZ^*, ΔA^*, and the trigonometric functions:

$$\begin{aligned} \Delta Z^{*m} &= a_1^m + a_2^m(\cos\alpha + \sin\alpha) + a_3^m \cos\alpha \, \sin\alpha \\ \Delta A^{*m} &= a_4^m(\cos\alpha - \sin\alpha) + a_5^m(\cos^2\alpha - \sin^2\alpha) \\ m &= l,\, g,\, r \end{aligned} \tag{6}$$

with the total changes given as the sum over the contributing mechanisms:

$$\begin{aligned} \Delta Z^* &= -\Delta Z^{*l} + \Delta Z^{*g} = a_1 + a_2(\cos\alpha + \sin\alpha) + a_3 \cos\alpha \, \sin\alpha \\ \Delta A^* &= -\Delta A^{*l} + \Delta A^{*g} + \Delta A^{*r} = a_4(\cos\alpha - \sin\alpha) + a_5(\cos^2\alpha - \sin^2\alpha) \\ a_i &= -a_i^l + a_i^g + a_i^r \end{aligned} \tag{7}$$

The results in Fig. 5 verify the accuracy of the expressions in Eq. 6 in fitting the variation of ΔZ^{*m} and ΔA^{*m} with strain probe direction α for the sample with initial coordination number of $Z_0 = 4.10$. Only a single coefficient, E^r, with the relatively constant value of 2.7, is required to represent the variation of fabric tensor due contact reorientation ΔF_{ij}^r, since no coordination number change is associated with contact reorientation, and the variation of ΔA^{*r} is accurately fitted with the first-order harmonic term, as demonstrated in Fig. 5(c).

By definition, incremental linearity for fabric evolution is obtained where a symmetry around $\alpha = 135°$ is observed, i.e. $\Delta\boldsymbol{F}(\alpha) = -\Delta\boldsymbol{F}(-\alpha)$. Therefore, based on the expressions in Eq. 6, an incrementally linear fabric response is obtained whenever all the following conditions are met:

1. The rate of change in coordination number due to contact loss in isotropic extension is equal to the rate of change in coordination number due to contact gain in isotropic compression.
2. The rates of change in coordination number due to contact loss and contact gain are equal in pure shear.
3. The maximum rate of change of anisotropy is obtained in pure shear.

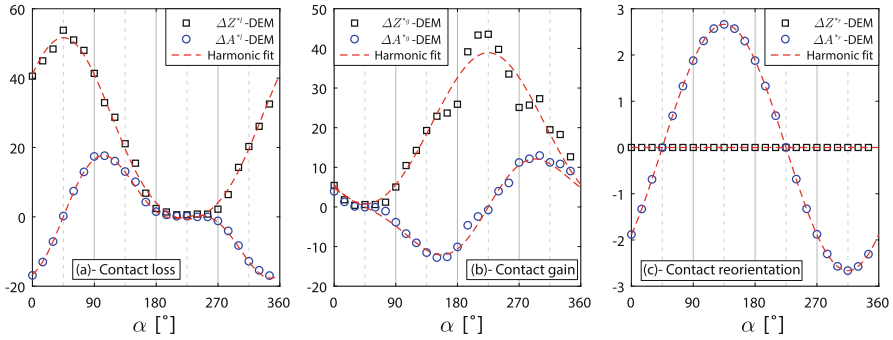

Fig. 5. Accuracy of the expressions in Eq. 6 in representing fabric change due to contact loss (left), contact gain (middle), and contact reorientation (right), for the sample with initial coordination number $Z_0 = 4.10$.

It is clear from the results in Fig. 4 that none of the above three conditions is satisfied, with the deviation from the first condition being the largest. The observed incrementally nonlinear evolution of fabric is particularly intriguing remembering that it occurs in a predominantly elastic deformation regime.

A more quantitative assessment of the incremental nonlinearity of fabric evolution is presented in Fig. 6 where the variation of coefficients in Eq. 7 with initial coordination number is given. Following the three above-mentioned requirements for incremental nonlinearity, the non-zero variables a_1, a_3, and a_5 point towards an incrementally nonlinear evolution of fabric with strain increments. Moreover, based on Eq. 7, the fact that $a_5 < a_3$ indicates that the deviation from incremental linearity is more significant for the deviatoric part of fabric tensor, ΔA^* compared to its spherical part, ΔZ^*. It is also important to notice that the changes in fabric scale with initial coordination number as suggested by the relatively linear trends in Fig. 6.

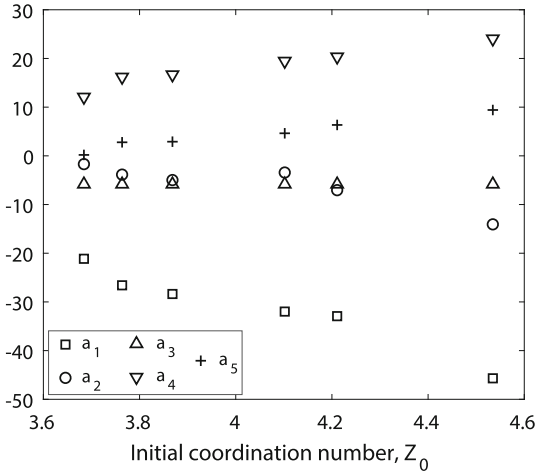

Fig. 6. Variation of coefficients describing the total fabric change in Eq. 7 with initial coordination number Z_0.

Such a dependency on the direction of loading further is consistent with the directional dependency of plastic flow rule [33] and constitutive models embedding such incremental nonlinearity [7,8,20].

4 Conclusions

Two-dimensional DEM simulations of initially isotropic systems have been performed to study the stress and fabric responses of granular media to strain probing. While the stress response remains incrementally linear and elastic, intriguingly, the fabric changes exhibit strong dependence on the strain probe direction, and hence incremental nonlinearity. Such an incrementally nonlinear evolution of the fabric response can only develop further to serve as a precursor to the elasto-plasticity of anisotropic granular assemblies.

To further explore the nature of fabric changes, the contributions of each of contact gain, loss, and reorientation mechanisms have been separately studied. As intuitively expected, the contribution of contact loss and gain are seen to be dominant in extensional and compressive probes, respectively. The contribution of contact reorientation is consistently negligible compared to the other two components.

As the main conclusions, the following qualitative observations have been made regarding the nature of fabric evolution:

1. In isotropic compression the rate of change in coordination number due to contact loss is very small, while the isotropic extension contact gain is very small.
2. The rate of change in anisotropy is not largest in pure shear, but in a probe direction that involves shear *and* extension.
3. The rate of contact loss in isotropic extension is larger than the rate of contact gain in isotropic compression. It is this difference that ultimately forms the primary origin of the incremental nonlinearity of fabric response to strain probing.
4. The parameters expressing the rate of change in the above-mentioned characteristic directions scale almost linearly with initial coordination number of the samples.

The results indicate that further studies, with wider ranges of conditions, are required to clearly explain the evolution of contact fabric and its role in driving the mechanical response of granular materials, especially in three-dimensional conditions. It will especially be interesting to study the fabric evolution in initially anisotropic configurations, for which, interrelations are expected between lost and gained contacts distributions, as our preliminary results show.

Finally, the observations in this study show that, as it stands, the issue of 'microstructure-motivated' elasticity is an open question, with more detailed investigations required to delineate the relation between fabric evolution and stress-strain response.

Acknowledgements. Research funding jointly provided by the Natural Sciences and Engineering Research Council of Canada and Foundation Computer Modelling Group (now Energi Solutions Ltd.) is gratefully acknowledged. This work was initiated during a short research visit at the University of Twente, the Netherlands, by the first author. Sincere gratitude is due to the University of Twente for providing an enriching and stimulating environment for this work, which has subsequently flourished into this manuscript.

References

1. Azéma, E., Radjai, F., Saussine, G.: Quasistatic rheology, force transmission and fabric properties of a packing of irregular polyhedral particles. Mech. Mater. **41**(6), 729–741 (2009)
2. Bagi, K.: Analysis of microstructural strain tensors for granular assemblies. Int. J. Solids Struct. **43**(10), 3166–3184 (2006)
3. Bardet, J.P.: Numerical simulations of the incremental responses of idealized granular materials. Int. J. Plast. **10**(8), 879–908 (1994)
4. Bashir, Y.M., Goddard, J.D.: A novel simulation method for the quasi-static mechanics of granular assemblages. J. Rheol. **35**(5), 849–885 (1991)
5. Calvetti, F., Viggiani, G., Tamagnini, C.: A numerical investigation of the incremental behavior of granular soils. Riv. Ital. Geotec. **37**(3), 11–29 (2003)
6. Calvetti, F., Combe, G., Lanier, J.: Experimental micromechanical analysis of a 2D granular material: relation between structure evolution and loading path. Mech. Cohesive-frictional Mater. **2**(2), 121–163 (1997)
7. Darve, F.: The expression of rheological laws in incremental form and the main classes of constitutive equations. In: Geomaterials: Constitutive Equations and Modelling, pp. 123–148 (1990)
8. Darve, F., Nicot, F.: On incremental non-linearity in granular media: phenomenological and multi-scale views (Part I). Int. J. Numer. Anal. Meth. Geomech. **29**(14), 1387–1409 (2005)
9. Drescher, A., De Jong, G.D.J.: Photoelastic verification of a mechanical model for the flow of a granular material. J. Mech. Phys. Solids **20**(5), 337–340 (1972)
10. Gao, Z., Zhao, J.: A non-coaxial critical-state model for sand accounting for fabric anisotropy and fabric evolution. Int. J. Solids Struct. **106–107**, 200–212 (2017)
11. Gudehus, G.: A comparison of some constitutive laws for soils under radially symmetric loading and unloading. Can. Geotech. J. **20**, 502–516 (1979)
12. Ken-Ichi, K.: Distribution of directional data and fabric tensors. Int. J. Eng. Sci. **22**(2), 149–164 (1984)
13. Kruyt, N.P.: Micromechanical study of fabric evolution in quasi-static deformation of granular materials. Mech. Mater. **44**, 120–129 (2012)
14. Kruyt, N.P., Rothenburg, L.: Micromechanical definition of the strain tensor for granular materials. J. Appl. Mech. **118**, 706–711 (1996)
15. Kruyt, N.P., Rothenburg, L.: Shear strength, dilatancy, energy and dissipation in quasi-static deformation of granular materials. J. Stat. Mech: Theory Exp. **2006**(07), P07021 (2006)
16. Kruyt, N.P., Rothenburg, L.: A micromechanical study of dilatancy of granular materials. J. Mech. Phys. Solids **95**, 411–427 (2016)
17. Li, X.S., Dafalias, Y.F.: Constitutive modeling of inherently anisotropic sand behavior. J. Geotech. Geoenvironmental Eng. **128**(10), 868–880 (2002)

18. Li, X.S., Dafalias, Y.F.: Anisotropic critical state theory: role of fabric. J. Eng. Mech. **138**(3), 263–275 (2011)
19. Love, A.E.H.: A Treatise on the Mathematical Theory of Elasticity. Cambridge University Press, Cambridge (1927)
20. Nicot, F., Darve, F.: Basic features of plastic strains: from micro-mechanics to incrementally nonlinear models. Int. J. Plas. **23**(9), 1555–1588 (2007)
21. Oda, M., Nemat-Nasser, S., Mehrabadi, M.M.: A statistical study of fabric in a random assembly of spherical granules. Int. J. Numer. Anal. Meth. Geomech. **6**(1), 77–94 (1982)
22. Oda, M.: Initial fabrics and their relations to mechanical properties of granular material. Soils Found. **12**(1), 17–36 (1972)
23. Pouragha, M., Wan, R.: Strain in granular media: a probabilistic approach to Dirichlet tessellation. J. Eng. Mech. **143**, C4016002 (2016)
24. Pouragha, M., Wan, R., Hadda, N.: A microstructural plastic potential for granular materials. In: Geomechanics from Micro to Macro, pp. 661–665 (2014)
25. Pouragha, M., Wan, R.: Non-dissipative structural evolutions in granular materials within the small strain range. Int. J. Solids Struct. **110**, 94–105 (2017)
26. Pouragha, M., Wan, R.: On elastic deformations and decomposition of strain in granular media. Int. J. Solids Struct. **138**, 97–108 (2018)
27. Radjai, F., Troadec, H., Roux, S.: Key features of granular plasticity. In Granular Materials: Fundamentals and Applications, pp. 157–184. Royal Society of Chemistry London, London (2004)
28. Rothenburg, L., Kruyt, N.P.: Critical state and evolution of coordination number in simulated granular materials. Int. J. Solids Struct. **41**(21), 5763–5774 (2004)
29. Rothenburg, L., Selvadurai, A.P.S.: A micromechanical definition of the Cauchy stress tensor for particulate media. In: Mechanics of Structured Media, pp. 469–486 (1981)
30. Rothenburg, L., Bathurst, R.J.: Analytical study of induced anisotropy in idealized granular materials. Géotechnique **39**(4), 601–614 (1989)
31. Satake, M.: Constitution of mechanics of granular materials through the graph theory. In: Proceedings of U.S.-Japan Seminar on Continuum Mechanical and Statistical Approaches in the Mechanics of Granular Materials Sendai, pp. 203–215 (1978)
32. Tobita, Y.: Fabric tensors in constitutive equations for granular materials. Soils Found. **29**(4), 91–104 (1989)
33. Wan, R., Pinheiro, M.: On the validity of the flow rule postulate for geomaterials. Int. J. Numer. Anal. Meth. Geomech. **38**(8), 863–880 (2014)
34. Wan, R., Pinheiro, M.: Fabric and connectivity as field descriptors for deformations in granular media. Continuum Mech. Thermodyn. **27**(1–2), 243–259 (2014)
35. Wan, R., Guo, J.: Drained cyclic behavior of sand with fabric dependence. J. Eng. Mech. **127**(11), 1106–1116 (2001)
36. Weber, J.: Recherches concernant les contraintes intergranulaires dans les milieux pulvérulents. Bul. Liaison P. et Ch **2**(64), 170 (1966)
37. Zhu, H.N., Mehrabadi, M.M., Massoudi, M.: Three-dimensional constitutive relations for granular materials based on the dilatant double shearing mechanism and the concept of fabric. Int. J. Plast. **22**(5), 826–857 (2006)